

# Low-voltage, high speed, compact silicon modulator for BPSK modulation

Tiantian Li,<sup>1</sup> Junlong Zhang,<sup>1</sup> Huaxiang Yi,<sup>1</sup> Wei Tan,<sup>1</sup> Qifeng Long,<sup>1</sup>  
Zhiping Zhou,<sup>1,2</sup> Xingjun Wang,<sup>1,\*</sup> and Hequan Wu<sup>1</sup>

<sup>1</sup>State Key Laboratory of Advanced Optical Communication Systems and Networks, School of Electronics Engineering and Computer Science, Peking University, Beijing, 100871, China

<sup>2</sup>xjwang@pku.edu.cn

\*zjzhou@pku.edu.cn;

**Abstract:** A low voltage, high speed, compact silicon Mach-Zehnder Interferometer (MZI) modulator for Binary Phase Shift Keying (BPSK) modulation has been demonstrated. High modulation efficiency,  $V_{\pi}L_{\pi}$  equals to 0.45V·cm, was obtained in a 1mm length device owing to a higher doping concentration and low-loss traveling-wave electrode. 25Gb/s non-return-to-zero(NRZ)-BPSK with 6V<sub>pp</sub> RF driving signal was achieved. Driven by a very low 3V<sub>pp</sub> RF signal, the 10Gb/s NRZ-BPSK was also realized benefiting from the high modulation efficiency and the low-voltage driving scheme. The power consumption for the BPSK modulation was as low as 0.118W. These results prove that the silicon modulator is suitable for advanced communication system with low power consumption.

©2013 Optical Society of America

**OCIS codes:** (230.7408) Wavelength filtering devices; (060.1660) Coherent communications; (130.0250) Optoelectronics.

---

## References and links

1. P. J. Winzer and R.-J. Essiambre, "Advanced optical modulation formats," *Proc. IEEE* **94**(5), 952–985 (2006).
2. P. J. Winzer and R.-J. Essiambre, "Advanced Modulation Formats for High-Capacity Optical Transport Networks," *J. Lightwave Technol.* **24**(12), 4711–4728 (2006).
3. Z. Zhou, X. Wang, H. Yi, Z. Tu, W. Tan, Q. Long, M. Yin, and Y. Huang, "Silicon photonics for advanced optical communication systems," *Opt. Eng.* **52**(4), 045007 (2013).
4. G. Raybon and P. Winzer, "100Gb/s Challenges and Solutions," in *Optical Fiber Communication Conference* (Optical Society of America, 2008), paper OTuG1.
5. D. J. Thomson, F. Y. Gardes, J.-M. Fedeli, S. Zlatanovic, Y. Hu, B. P. P. Kuo, E. Myslivets, N. Alic, S. Radic, G. Z. Mashanovich, and G. T. Reed, "50-Gb/s Silicon Optical Modulator," *IEEE Photon. Technol. Lett.* **24**(4), 234–236 (2012).
6. J. Ding, H. Chen, L. Yang, L. Zhang, R. Ji, Y. Tian, W. Zhu, Y. Lu, P. Zhou, R. Min, and M. Yu, "Ultra-low-power carrier-depletion Mach-Zehnder silicon optical modulator," *Opt. Express* **20**(7), 7081–7087 (2012).
7. H. Xu, Z. Li, Y. Zhu, Y. Li, Y. Yu, and J. Yu, "Silicon optical modulator with integrated grating couplers based on 0.18- $\mu$ m complementary metal oxide semiconductor technology," *Opt. Eng.* **50**(4), 044001 (2011).
8. H. Yi, Q. Long, W. Tan, L. Li, X. Wang, and Z. Zhou, "Demonstration of low power penalty of silicon Mach-Zehnder modulator in long-haul transmission," *Opt. Express* **20**(25), 27562–27568 (2012).
9. K. Padmaraju, N. Ophir, Q. Xu, B. Schmidt, J. Shakya, S. Manapatruni, M. Lipson, and K. Bergman, "Error-Free Transmission of DPSK at 5 Gb/s Using a Silicon Microring Modulator," in *European Conference and Exposition on Optical Communications* (Optical Society of America, 2011), Th.12.LeSaleve.2.
10. K. Goi, K. Oda, H. Kusaka, Y. Terada, K. Ogawa, T.-Y. Liow, X. Tu, G.-Q. Lo, and D.-L. Kwong, "11-Gb/s 80-km Transmission Performance of Zero-Chirp Silicon Mach-Zehnder Modulator," *Opt. Express* **20**(26), B350–B356 (2012).
11. P. Dong, L. Chen, C. Xie, L. L. Buhl, and Y.-K. Chen, "50-Gb/s silicon quadrature phase-shift keying modulator," *Opt. Express* **20**(19), 21181–21186 (2012).
12. P. Dong, C. Xie, L. L. Buhl, and Y.-K. Chen, "Silicon Microring Modulators for Advanced Modulation Formats," in *Optical Fiber Communication Conference* (Optical Society of America, 2013), paper OW4J.2.
13. P. Dong, C. Xie, L. Chen, L. L. Buhl, and Y.-K. Chen, "112-Gb/s Monolithic PDM-QPSK Modulator in Silicon," *Opt. Express* **20**(26), B624–B629 (2012).
14. K. Goi, H. Kusaka, A. Oka, Y. Terada, K. Ogawa, T.-Y. Liow, X. Tu, G. Lo, and D.-L. Kwong, "DQPSK/QPSK Modulation at 40-60 Gb/s using Low-Loss Nested Silicon Mach-Zehnder Modulator," in *Optical Fiber Communication Conference* (Optical Society of America, 2013), paper OW4J.4.
15. D. J. Thomson, Y. Hu, G. T. Reed, and J.-M. Fedeli, "Low Loss MMI Couplers for High Performance MZI

- Modulators,” *IEEE Photon. Technol. Lett.* **22**(20), 1485–1487 (2010).
16. J. Ding, H. Chen, L. Yang, L. Zhang, R. Ji, Y. Tian, W. Zhu, Y. Lu, P. Zhou, and R. Min, “Low-voltage, high-extinction-ratio, Mach-Zehnder silicon optical modulator for CMOS-compatible integration,” *Opt. Express* **20**(3), 3209–3218 (2012).
  17. K. Goi, K. Oda, H. Kusaka, K. Ogawa, T.-Y. Liow, X. Tu, and G.-Q. Lo, “20-Gbps BPSK silicon Mach-Zehnder modulator with excellent chirp-free performance,” in *Proceedings of OptoElectronics and Communications Conference*, pp. 238–239.
  18. R. Schmogrow, B. Nebendahl, M. Winter, A. Josten, D. Hillerkuss, S. Koenig, J. Meyer, M. Dreschmann, M. Huebner, C. Koos, J. Becker, W. Freude, and J. Leuthold, “Error Vector Magnitude as a Performance Measure for Advanced Modulation Formats,” *IEEE Photon. Technol. Lett.* **24**(1), 61–63 (2012).

## 1. Introduction

As the requirement for communication capacity increases, advanced modulation formats continue to attract great attention on account of their larger information capacity [1–4]. M-PSK and M-QAM are typical examples of advanced modulation formats, in which the information is carried not only by the amplitude but also the phase. High performance amplitude modulations have been demonstrated by using silicon modulators. Excellent properties of high speed [5], low-voltage [6] and compact size [7] were obtained. Moreover, negative chirp property which helps the long-haul transmission was also reported recently [8]. For basic phase modulation, BPSK has previously been generated on a silicon microring modulator [9], while 22.3Gb/s BPSK has recently been demonstrated on silicon MZI modulator under a  $7V_{pp}$  driving voltage in 4mm length phase shifter [10]. Meanwhile quadrature phase shift keying (QPSK) using two nested silicon MZI modulators [11] or microring modulators [12] has also been reported. 50Gb/s QPSK was firstly obtained in 2012 under  $12V_{pp}$  in approximately 5mm length single-drive phase shifter [11]. 112Gb/s PDM-QPSK has also been demonstrated [13], and dual-drive 64Gb/s QPSK under a driving voltage of  $8V_{pp}$  in shorter 3mm length phase shifter has also been realized in 2013 [14]. However, in the aforementioned works, the driving voltage of the MZI modulator is still higher than  $6V_{pp}$ , and the length is larger than 3mm. The driving voltage is higher than the conventional driving voltage in CMOS and consumes more power, limiting the application in large capacity communication systems. The large footprint is also unsuitable for monolithic integration with other devices. In this paper, we present high speed BPSK modulation based on a compact silicon MZI modulator with low driving voltage. Owing to the high modulation efficiency and the driving scheme of the silicon MZI modulator, we firstly observed 25Gb/s NRZ-BPSK under  $6V_{pp}$  in 1mm length phase shifter, and then realized 10Gb/s BPSK with very low  $3V_{pp}$  driving voltage and a length of 1mm. The power consumption has been significantly reduced.

## 2. BPSK modulation theory in silicon MZI modulator

The input beam defined as  $E_{in}$  is evenly split into MZI modulator as  $A_1E_{in}$  and  $A_2E_{in}$ .  $A_1$   $A_2$  is the propagation factor which is influenced by the splitting ratio of MMIs and the propagation loss on the two modulated arms. Since we mainly focus on the signal phase, the propagation factors in both arms are assumed to be identical and the loss is ignored for simplicity ( $A_1 = A_2 = 1/2$ ). After going through the phase shifters in the silicon MZI modulator, the optical beams are expressed as  $E_{in} \exp(j\phi_1)/2$  and  $E_{in} \exp(j\phi_2 + j\phi)/2$ , where  $\phi_1$  and  $\phi_2$  are the shifted phases in arm1 and arm2 induced by the driving signal, and  $\phi$  is the initial phase difference between the arms. Hence, the output can be obtained as:

$$E_{out} = E_1 + E_2 = \frac{E_{in}}{2} \exp(j\phi_1) + \frac{E_{in}}{2} \exp(j\phi_2 + j\phi). \quad (1)$$

Since in the BPSK modulation formats,  $\phi = \pi$ , the formula can be simplified as:

$$E_{out} = E_{in} \sin\left(\frac{\phi_1 - \phi_2}{2}\right) \exp j\left(\frac{\phi_1 + \phi_2 + \pi}{2}\right). \quad (2)$$

The silicon modulator works in the push-pull driving mode. Due to the carrier depletion structure, the driving voltages should remain negative. In the signal “1” state, arm1 is driven by  $-V_{cc}$  while arm2 is driven by 0V. The corresponding phase shift in arm1 and arm2

is  $\phi_1 = \varphi$  and  $\phi_2 = 0$ , and  $E_{out1}$  is rewritten as  $E_{in} \sin(\varphi/2) \exp j(\varphi/2 + \pi/2)$ . In the signal “0” state, arm 1 is driven by 0V while arm2 is driven by  $-V_{cc}$ . The corresponding phase shift is  $\phi_1 = 0$  and  $\phi_2 = \varphi$ , and  $E_{out2}$  is rewritten as  $E_{in} \sin(-\varphi/2) \exp j(\varphi/2 + \pi/2)$ . The calculated output is shown in Fig. 1.  $V_{\pi}$  is the driving voltage which produces  $\pi$  phase shift. When  $V_{cc} = V_{\pi}$ , we can obtain the ideal BPSK constellation diagram with both signal dots on the x axis, where  $\pi$  is the phase difference between them. When  $V_{cc} < V_{\pi}$ , neither signal dots lies on the x axis and there is an initial angle  $(\pi - \varphi)/2$ , while the  $\pi$  phase difference still exists between the “1” and “0” states. Therefore, when the driving voltage is less than  $V_{\pi}$  with the initial angle correction, the BPSK signal can be produced with the silicon MZI modulator in the push-pull driving mode. Furthermore, the initial angle of the BPSK signal can be utilized as pre-distortion to compensate the angle rotation after long-haul transmission. It is suggested that the low-voltage driving scheme causes the smaller optical amplitude due to the coefficient of  $\sin(\varphi/2)$  and leads to excess optical loss. Consequently the OSNR is influenced by the low-voltage driving scheme. So for practical application, there is a trade-off between the requisite signal quality and driving voltage.

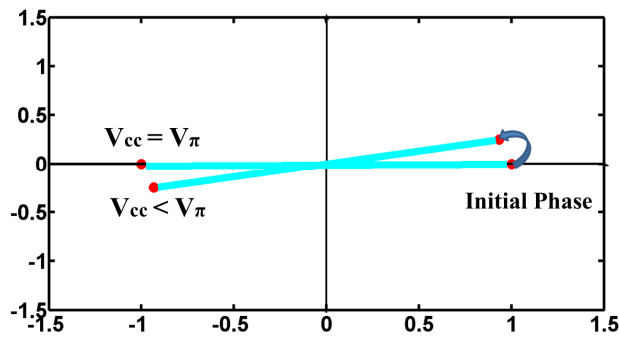


Fig. 1. BPSK constellation diagram with different driving voltage.

### 3. Design and experimental setup

Figure 2(a) shows a cross-section of the phase shifters in the silicon MZI modulator. The phase shifter is based on a rib waveguide with a width of 600nm. The height of the slab is 60nm and the total height of the rib waveguide is 220nm. In order to increase the modulation efficiency, the doping concentration is designed to be  $5 \times 10^{17}/\text{cm}^3$  for the p-type region and  $1 \times 10^{18}/\text{cm}^3$  for the n-type region. Moreover the p-type region is offset 100nm to the right of the center of the waveguide to enlarge the overlap between p-type region and light field. There is a 50nm intrinsic gap between the p-type and n-type regions in the PN junction, which is introduced to decrease the capacitor in order to exploit the bandwidth of the modulator. The distance between the edge of the rib and the heavy doping area is  $0.5\mu\text{m}$ . The doping concentration of the P + + and N + + regions are both  $1 \times 10^{20}/\text{cm}^3$  for a good ohmic contact. The silicon MZI modulator is designed with 1mm phase shifters. The length difference is  $100\mu\text{m}$  between the two arms and two  $1 \times 2$  multimode interferometers (MMI) are used to split and recombine the optical beam in the MZI modulator [15]. A coplanar waveguide (CPW) is introduced to drive the phase shifter as shown in Fig. 2(b). The width of the signal(S) electrodes is  $4\mu\text{m}$ . The distance between the ground (G) and S electrodes is  $6.5\mu\text{m}$ . The characteristic impedance of the CPW is calculated to be approximately  $38\Omega$  using HFSS software [16]. Four integrated termination resistances are fabricated approximately  $76\Omega$  between every G and S electrode to reduce the microwave reflection.

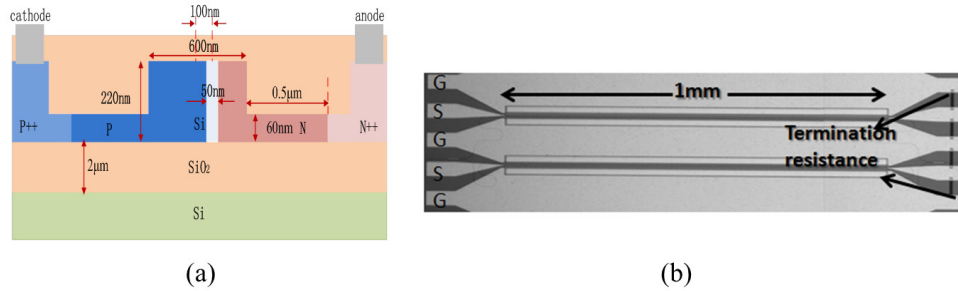


Fig. 2. Schematic diagram of the device: (a) Cross-section diagram, (b) Optical micrograph of the modulator with a CPW electrode.

The measurement setup for the BPSK modulation is shown in Fig. 3. A continuous-wave (CW) laser was employed to generate the optical signal. The polarization was set to TE by a deterministic polarization controller (DPC). Due to the large insertion loss, the first EDFA after DPC was employed to ensure that enough power had input to the modulator. The differential electric signals were generated by a Pulse Pattern Generator (PPG) and then amplified by a pair of 28GHz broadband amplifiers. Combining the Radio Frequency (RF) signal and the DC bias, both of the modulator's two arms were driven in push-pull driving mode with the differential signals. The second EDFA before the receiver was employed to amplify the modulated signal to satisfy the sensitivity of the commercial coherent optical receiver (EXFO PSO-200).

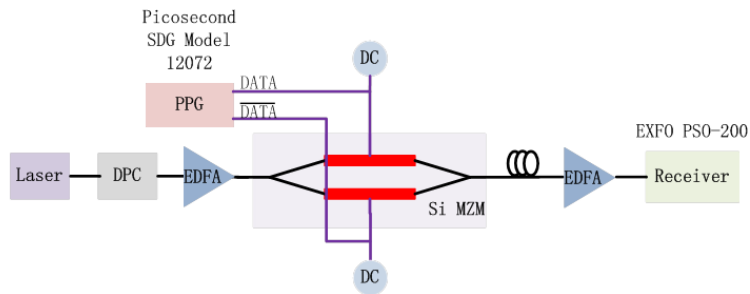


Fig. 3. Measurement setup for the BPSK modulation.

#### 4. Measurement and discussion

Firstly, the static spectrum was measured as a function of  $V_{\text{bias}}$ . For the 1mm length modulator, the  $\pi$  phase shift voltage ( $V_{\pi}$ ) for one modulated arm is approximately 4.5V as shown in Fig. 4(a), and both of the on-off extinction ratios are larger than 35dB. The  $V_{\pi}L_{\pi}$  for the modulator is calculated to be approximately  $0.45V \cdot \text{cm}$ . The modulation efficiency is less than half of other groups' work based on the traditional carrier depletion structure [6, 11, 14]. The high modulation efficiency benefits from the high doping level, optimized PN junction and the design of the CPW traveling-wave electrode. The high modulation efficiency is essential to realize BPSK modulation with compact size and low-voltage. However, because of the higher doping level, there is a higher optical propagation loss. The propagation loss of the Si MZI modulator is approximately 8dB included 6.4dB in 1mm phase shifter and 0.8dB per MMI.

The S-parameter of the MZI modulator was measured with a vector network analyzer (VNA) (Anritsu MS4640A). A CW laser, DC electrical source, RF GSGSG probe and bias-Tee were employed. The VNA cooperated with the bias-Tee, RF cable and all the adaptors were calibrated before the measurement with the calibration kit. Figure 4(b) shows the measured electro-optical (E-O) modulation response under zero bias voltage. The optical 3-dB bandwidth is larger than 13GHz, which implies highly velocity-matching between the electrical and optical signal in the low-loss CPW traveling-wave electrode.

The 50nm intrinsic region and the 1mm length are also helpful in achieving the 13GHz 3-dB bandwidth due to the reduced capacity and loss. In order to realize high modulation efficiency, the traveling-wave electrode was designed with larger characteristic impedance approaching  $50\Omega$  to reduce the reflection loss caused by the mismatching between the traveling-wave electrode ( $38\Omega$ ) and the probe ( $50\Omega$ ). However it was hard to further reduce the microwave propagation loss on the traveling-wave electrode at the same time which mainly limited the optical bandwidth.

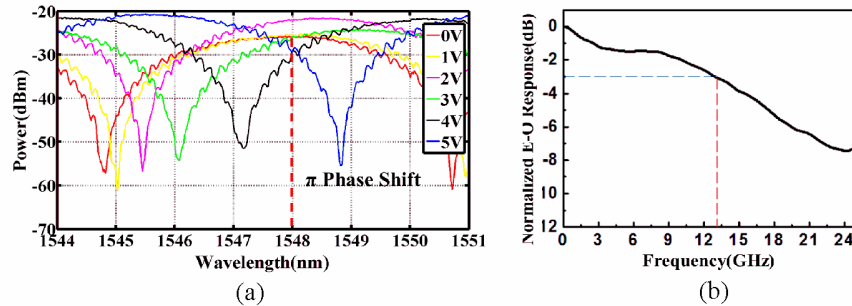


Fig. 4. (a) Static spectrum for different  $V_{\text{bias}}$ , (b) Measured E-O response of the 1mm MZI modulator.

The 1mm high efficiency device was adopted to generate high speed BPSK. A 100KHz narrow line width laser of 1550.51nm was employed to decrease the phase noise. The PPG generated a  $2^7-1$  pseudo-random bit sequence (PRBS). The differential RF signals were both amplified to 6V with DC bias of 3.9V and 2.6V. Data rates of 10Gb/s and 20Gb/s were demonstrated respectively under the same voltage. A data rate of 25Gb/s was demonstrated under  $6V_{\text{pp}}$  with a DC bias of 3.2V and 3.1V. The Si MZI modulator was driven in push-pull driving mode. The modulated signals were received by the commercial coherent receiver and the results are shown in Fig. 5(a). The published advanced modulation formats realized by a silicon MZI modulator usually employ Q-factor to evaluate the signal quality [17]. However, error vector magnitude (EVM) is more suitable than Q-factor to evaluate the quality of the received BPSK signal, which describes the effective distance of the received complex symbol from its ideal position in the constellation diagram [18]. It is also related to the bit error rate (BER) and optical signal to noise ratio (OSNR) of the signal. In our experiment the EVM of the 10Gb/s BPSK constellation diagram is 16.7 with an OSNR of 16.9dB. According to the well-known relationship between EVM and BER [18], the corresponding BER is  $1 \times 10^{-10}$ . In this situation, the signal quality is comparable to the commercial  $\text{LiNbO}_3$  MZM in the inset of Fig. 5(a), whose EVM is 17.7 with an OSNR of 17.3dB under the 10Gb/s BPSK modulation. Under similar experimental condition, after increasing the data rate up to 20Gb/s, the EVM is 24.3 with an OSNR of 12.4dB. The corresponding BER is  $1 \times 10^{-8}$ . In the 25Gb/s data rate, we find that some distortion in the constellation diagram, which we attribute to the chirp due to the light asymmetry of the two arms. The chirp would become more obvious at high data rate. In this situation the EVM is 26.0 with a corresponding BER of  $1 \times 10^{-7}$ .

BPSK modulation under different driving voltages was also demonstrated. A CW laser with 1MHz line width was introduced at 1550.82nm. An amplified differential  $5.1V_{\text{pp}}$  and  $5.4V_{\text{pp}}$  RF signal with a DC bias of 2.6V was employed to drive each arm of the MZI modulator. Because of the light asymmetry caused by the fabrication error, the driving voltage of the two arms could not always be identical. We obtained the back-to-back eye diagram and constellation diagram from the commercial coherent receiver as shown in Fig. 5(b). The EVM of the 10Gb/s signal is 17.2 with an OSNR of 15.9dB. We then used an amplified  $4V_{\text{pp}}$  RF signal with DC bias of 3.1V and 3.6V at 1550.96nm. The EVM of the constellation diagram is 26.7 with an OSNR of 13.9dB. When the driving voltage decreased to  $3V_{\text{pp}}$  with DC bias of 1.5V, we could still obtain a clear eye diagram and constellation diagram. Because of the offline DSP of the commercial receiver, we obtained

the constellation diagram without rotation. The OSNR of the signal under 3V<sub>pp</sub> driving voltage is 11.4dB which is 4.5dB lower compared to when a 5V<sub>pp</sub> driving voltage is used, which is caused by the low-voltage driving. Although the OSNR is not that perfect, an EVM of 32.5 still can be acquired. And the corresponding BER is nearly  $1 \times 10^{-5}$ , which is lower than the forward error correction (FEC) threshold. It is possible to achieve error-free transmissions with FEC techniques. The quality of the received signal can still be improved using an optical band-pass filter (OBPF) after the second EDFA.

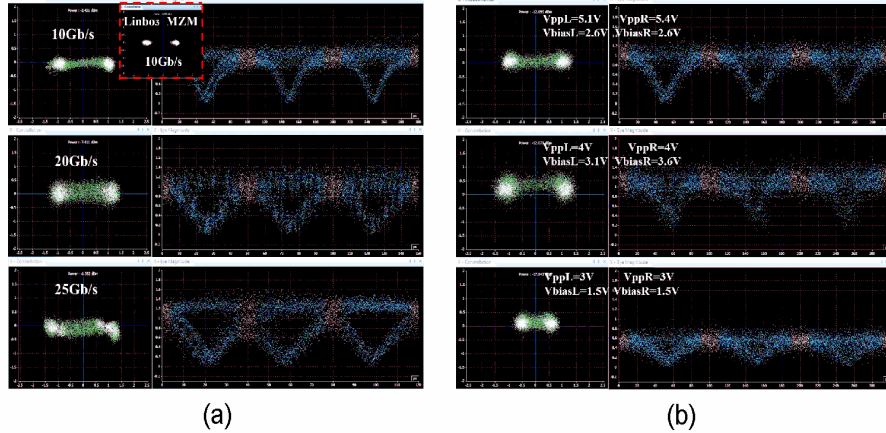


Fig. 5. The constellation diagrams and eye diagrams: (a) Different data rates of 10Gb/s, 20Gb/s and 25Gb/s, (b) 10Gb/s data rate under different driving voltages

We have successfully demodulated the BPSK signal under 5V<sub>pp</sub>, 4V<sub>pp</sub> and 3V<sub>pp</sub>, which are all smaller than V<sub>π</sub>. Based on previous theoretical analysis, a driving voltage of less than V<sub>π</sub> has been experimentally demonstrated. The power consumption can be reduced to 0.118W ( $P = 2 \times \left( \frac{1}{4} \cdot \frac{V_{pp}^2}{R} \right)$ ,  $V_{pp} = 3V$ ,  $R = 38\Omega$ ) [6]. When the modulator transmits the

continuous data 1 or 0 at 10Gb/s under a 3V<sub>pp</sub> driving voltage, the corresponding power efficiency is 11.8pJ/bit. Because of the high modulation efficiency and the low-voltage driving scheme in our work, the power consumption has been reduced.

## 5. Conclusion

We have demonstrated a high modulation efficiency silicon MZI modulator with V<sub>π</sub>L<sub>π</sub> equal to 0.45V·cm. The 25Gb/s BPSK modulation was obtained by employing a 1mm silicon MZI modulator. A minimum driving voltage of 3V<sub>pp</sub> was also demonstrated, which made the power efficiency decrease to 11.8pJ/bit at 10Gb/s BPSK modulation. Even higher power efficiency is predicted at higher data rates. The compact footprint and low power consumption make the silicon modulator more suitable for advanced modulation application. Furthermore, the initial phase, when V<sub>cc</sub> < V<sub>π</sub>, can act as the pre-distortion in long-haul transmission to compensate the rotation of the constellation diagram.

## Acknowledgments

This work is partially supported by the National High Technology Research and Development Program of China (863 Program) (Grant No. 2011AA010302), and National Natural Science Foundation of China (Grant No. 61205026).